NF-κB and Snail1a coordinate the cell cycle with gastrulation

Xiaolin Liu,[1,2] Sizhou Huang,[1,2] Jun Ma,[1,2] Chun Li,[1,2] Yaoguang Zhang,[1] and Lingfei Luo[1,2]

[1]Key Laboratory of Aquatic Organism Reproduction and Development, Ministry of Education, Key Laboratory of Aquatic Science of Chongqing, and [2]Laboratory of Molecular Developmental Biology, School of Life Science, Southwest University, Beibei, 400715 Chongqing, China

The cell cycle needs to strictly coordinate with developmental processes to ensure correct generation of the body plan and different tissues. However, the molecular mechanism underlying the coordination remains largely unknown. In this study, we investigate how the cell cycle coordinates gastrulation cell movements in zebrafish. We present a system to modulate the cell cycle in early zebrafish embryos by manipulating the geminin-Cdt1 balance. Alterations of the cell cycle change the apoptotic level during gastrulation, which correlates with the nuclear level of antiapoptotic nuclear factor κB (NF-κB). NF-κB associates with the *Snail1a* promoter region on the chromatin and directly activates Snail1a, an important factor controlling cell delamination, which is the initial step of mesendodermal cell movements during gastrulation. In effect, the cell cycle coordinates the delamination of mesendodermal cells through the transcription of *Snail1a*. Our results suggest a molecular mechanism by which NF-κB and Snail1a coordinate the cell cycle through gastrulation.

Introduction

During the developmental transition from a single-celled zygote to a mature biological organism, numerous cell division and differentiation events take place, resulting in embryonic growth and the formation of different tissues. Cell differentiation and tissue formation must be coordinated with the cell cycle to guarantee correct spatial and temporal generation of the body plan as well as functional organs. Gastrulation is an early developmental process leading to formation of three germ layers, endoderm, mesoderm, and ectoderm, involving a series of cellular movements (Stern, 2004). In zebrafish, gastrulation starts with internalization of mesendodermal progenitors in the dorsal/axial regions of the germ ring by single-cell delamination. Then, the delaminated cells start to migrate underneath the epiblast toward the animal pole as well as the midline, thus forming the mesendodermal cell layer (Warga and Kimmel, 1990; Montero and Heisenberg, 2004).

Snail, a zinc finger transcriptional repressor, is important for cell delamination and migration, which are critical mesendodermal cell movement events during gastrulation. Both *Drosophila snail* mutants and zebrafish embryos injected with a morpholino oligo against *Snail1a* (Snail1aMO) display severe defects in gastrulation cell movements (Ip and Gridley, 2002; Yamashita et al., 2004; Blanco et al., 2007). In *Drosophila*, Snail is activated by Twist, a basic helix-loop-helix transcription activator, and Dorsal, a maternal transcription factor that is the *Drosophila* homologue of the vertebrate nuclear factor κB (NF-κB) subunit p65/RelA (Jiang et al., 1991; Ip et al., 1992; Ip and Gridley, 2002).

After dissociation from the inhibitory IκB/cactus and subsequent nuclear translocation, NF-κB can activate not only *Snail* but also antiapoptotic factors like the Bcl-2 family in response to apoptotic stimuli (Zong et al., 1999). In most vertebrates, including zebrafish, apoptosis is not seen before gastrulation but thereafter plays a major role in shaping and sculpting the embryo (Negron and Lockshin, 2004; Penaloza et al., 2006). The nearly simultaneous appearance of apoptosis and gastrulation cell movements implies a possible molecular link between these two events. Actually, inhibition of NF-κB function with dominant-negative IκBα in zebrafish leads to defective notochord development (Correa et al., 2004).

Cdt1, a DNA replication initiation factor, is required for loading of the minichromosome maintenance (MCM) complex

Correspondence to Lingfei Luo: lluo@swu.edu.cn

Abbreviations used in this paper: bon, bonnie and clyde; CAT, chloramphenicol acetyl transferase; ChIP, chromatin immunoprecipitation; conMO, control morpholino; gsc, goosecoid; H3P, phosphorylated histone 3; hpf, hours post fertilization; MCM, minichromosome maintenance; mrGem, GemMO-resistant geminin; NF-κB, nuclear factor κB; ntl, no tail; Sn1-CAT, Snail1a promoter driving chloramphenicol acetyl transferase construct.

The Rockefeller University Press $30.00
J. Cell Biol. Vol. 184 No. 6 805–815
www.jcb.org/cgi/doi/10.1083/jcb.200806074

onto chromatin to assemble the prereplicative complex (Bell and Dutta, 2002). Once the DNA replication is initiated, DNA replication must remain inhibited within the same cell cycle to maintain the genetic stability of an organism. Geminin accumulates in the nucleus from early S phase to the end of mitosis and directly binds to Cdt1, sequestering Cdt1 from binding to the MCM complex and DNA, and preventing resynthesis of DNA (McGarry and Kirschner, 1998; Wohlschlegel et al., 2000; Tada et al., 2001; Yanagi et al., 2002). In higher eukaryotes, geminin serves as a major DNA replication safeguard (Melixetian and Helin, 2004), and the balance between geminin and Cdt1 levels is critical for cell cycle control (Saxena and Dutta, 2005). In *Xenopus laevis* egg extracts, the stoichiometry of the Cdt1-geminin balance regulates its activity (Lutzmann et al., 2006).

Progression through the cell cycle is incompatible with certain types of cell behavior like cell migration, adhesion, and changes in cell shape. In *Drosophila*, a serine/threonine kinase, Tribbles, inhibits the cell cycle in the prospective mesoderm by counteracting the activity of the protein phosphatase Cdc25/String. This Snail-dependent cell cycle inhibition allows cell shape changes important for mesodermal development (Grosshans and Wieschaus, 2000; Seher and Leptin, 2000). However, the molecular mechanism underlying the coordination of the cell cycle with gastrulation is unclear. In this study, we establish a system to modulate the cell cycle in early zebrafish embryos by manipulating the geminin-Cdt1 balance. Modulations of the cell cycle in gastrulating embryos alters patterns of apoptosis, which further corresponds to abnormal activation of NF-κB that has an antiapoptotic function. The abnormal level of nuclear and active NF-κB alters the transcription of *Snail1a*, thus leading to defects in cell delamination at the marginal zone. Because it is the initial step of mesendodermal cell movements during gastrulation, defective cell delamination results in aberrant mesendodermal cell movements. Our results suggest a mechanism underlying the coordination of the cell cycle with mesendodermal cell movements during gastrulation, involving apoptosis, NF-κB, and Snail1a.

Results

The cell cycle is modulated by manipulation of the geminin-Cdt1 balance

To investigate the mechanism underlying coordination of the cell cycle with gastrulation, we first established a tool to manipulate the cell cycle in gastrulating embryos. cDNAs encoding zebrafish geminin and Cdt1 were isolated using cDNA prepared from the shield stage zebrafish embryos. Zebrafish Cdt1 has 678 amino acids with 49%, 41%, and 42% respective identity to the proteins in *Xenopus*, mouse, and human, whereas zebrafish geminin consists of 241 amino acids with 54%, 46%, 39%, and 39% identity to geminin proteins in medaka, *Xenopus*, mouse, and human, respectively (Fig. S1, A and B). At the shield stage, geminin transcripts were uniformly detected, whereas Cdt1 was more enriched in the dorsal region of the embryo (Fig. S2), suggesting that cells in the dorsal region might possess higher proliferative activity.

Overexpression and knockdown of geminin in medaka fish were previously reported to decrease and increase the number of mitotically active cells, respectively (Del Bene et al., 2004). To analyze the effect of manipulating the geminin-Cdt1 balance on the cell cycle in gastrulating zebrafish embryos, geminin and Cdt1 levels were altered by mRNA overexpression or knockdown with specific antisense morpholino oligos (Fig. S3 A, GemMO and Cdt1MO). Mitotically active cells were marked using antibodies against phosphorylated histone 3 (H3P) at the shield stage (Fig. 1, A–E). In contrast to embryos injected with a control morpholino (ConMO), injection of GemMO or *Cdt1* mRNA increased the number of mitotically active cells. On the contrary, geminin overexpression or Cdt1 knockdown decreased the number of mitotically active cells. To investigate whether these effects on the cell cycle were dependent on direct interaction

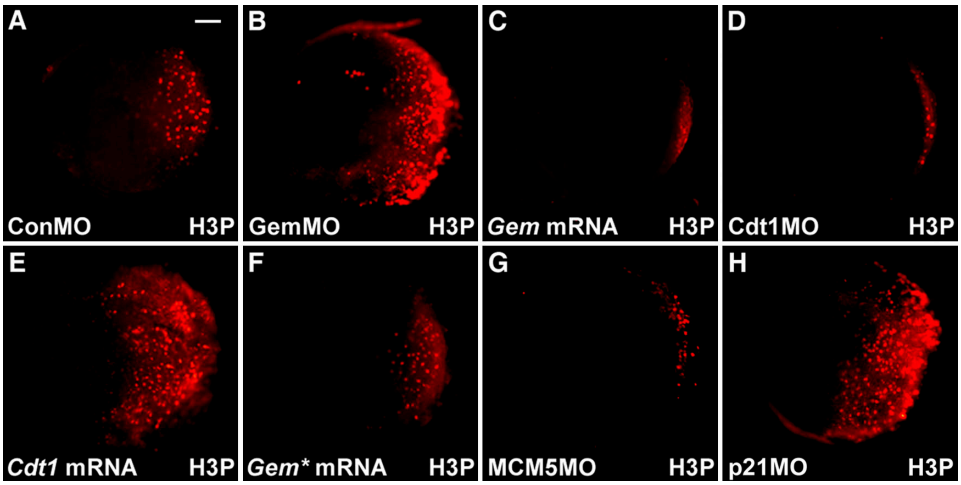

Figure 1. **Manipulations of the geminin–Cdt1 balance, MCM5, or p21 function result in modulations of the cell cycle.** (A–F) Geminin and Cdt1 reciprocally direct the cell cycle. In contrast to embryos injected with ConMO (A) or *Gem** mRNA (F), the number of mitotically active cells marked by H3P staining was increased in GemMO (B)-, *Cdt1* mRNA (E)–, or p21MO (H)-injected embryos but decreased in *geminin* (*Gem*) mRNA (C)–, Cdt1MO (D)-, or MCM5MO (G)-injected embryos. The shield stage embryos were viewed from the animal pole with the dorsal side to the right. Bar, 100 µm.

of geminin and Cdt1, a full-length mutated geminin (Gem*), in which five highly conserved amino acids responsible for Cdt1 interaction (Fig. S1 B, asterisks; Lee et al., 2004; Saxena et al., 2004) were mutated to alanine, was constructed (Fig. S3 B). The number of H3P-positive cells in embryos injected with *Gem** mRNA was similar to that in the control (Fig. 1 F). Knockdown of another cell cycle regulator, MCM protein 5 (MCM5), a subunit of the MCM complex that is required for the assembly of the prereplication complex, resulted in a decreased number of H3P-positive cells (Fig. 1 G). Knockdown of p21, a CDK inhibitor, offered a completely different means to modulate the cell cycle (Fig. 1 H). Similar cell cycle regulatory effects were observed in the 70% epiboly and 90% epiboly stage embryos when the geminin–Cdt1 balance was manipulated (not depicted). These results indicate that the balanced interaction of geminin and Cdt1 is critical for cell cycle regulation, such that perturbation of the balance allows positive and negative modulations of the cell cycle in gastrulating embryos.

Modulation of the cell cycle leads to defective mesendodermal cell movements by affecting cell delamination

To address the effect of cell cycle modulation on zebrafish gastrulation, we examined the phenotype of embryos injected with GemMO. At the bud stage, the end of gastrulation, GemMO injection resulted in reduced extension of the anterior-posterior axis (Fig. 2, A and B) and was specifically rescued by coinjection of a GemMO-resistant *geminin* (*mrGem*) mRNA encoding full-length geminin protein but with a nine-base mismatch to GemMO (not depicted). The shortened anterior-posterior axis in embryos injected with GemMO suggested defective mesendodermal cell movements. This assumption was tested by examining the position of *goosecoid* (*gsc*)-expressing anterior-most axial mesendodermal cells that will give rise to the prechordal plate. At the 80% epiboly stage, the anterior boundary of prechordal plate precursor cells in embryos injected with GemMO or *Cdt1* mRNA was posterior to that in controls (Fig. 2, C, D, and H).

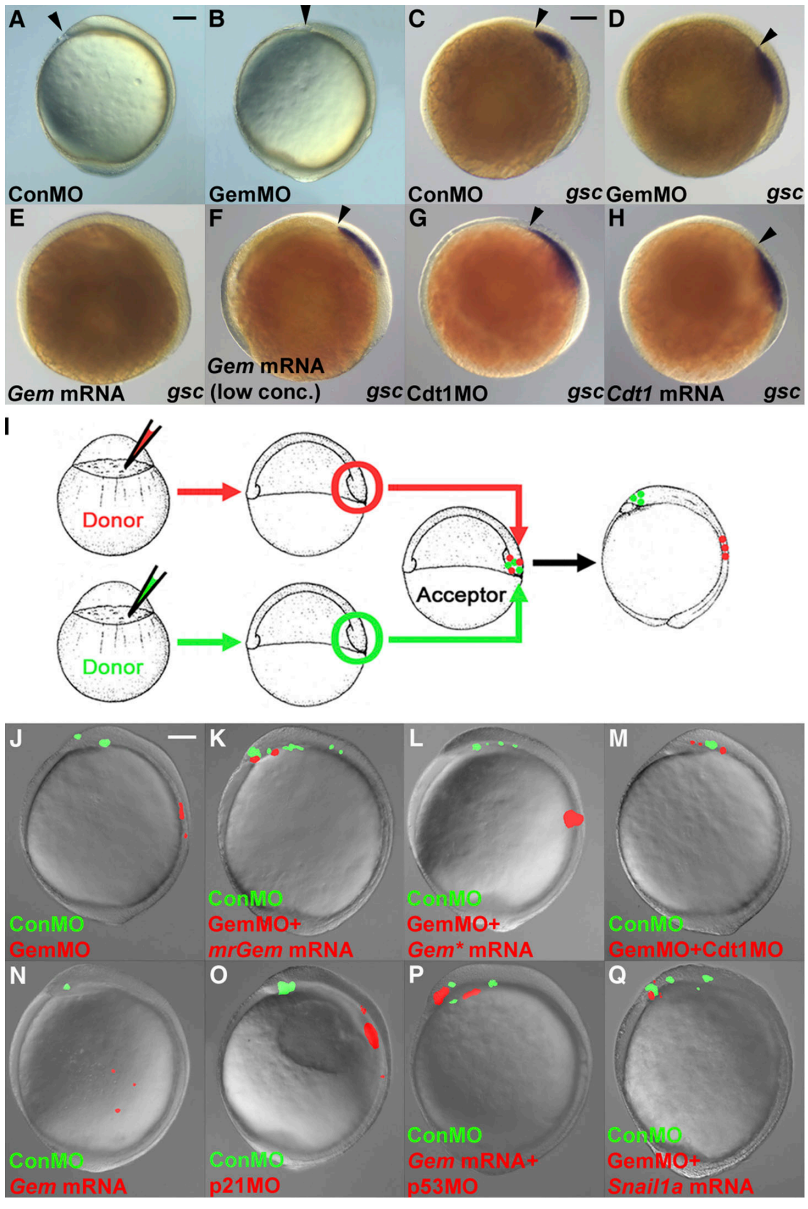

Figure 2. **Modulations of the cell cycle change mesendodermal cell movements.** (A and B) Gastrulation phenotype caused by GemMO. Note the shortened body axis in embryos injected with GemMO. Arrowheads mark the anterior boundary of hypoblast. (C–H) Modulations of the cell cycle change the position of *gsc*-expressing cells in the 80% epiboly embryos. Arrowheads mark the anterior boundary of the *gsc*-expressing domain. (I) Schematic representation of the cotransplantation assay. Green and red indicate transplanted green and red fluorescent donor cells, respectively. (J–Q) The cell cycle coordinates mesendodermal cell movements through apoptosis and Snail1a. Similar to the transplanted cells with p21 knocked down (O), GemMO led to delayed movements of transplanted cells (J), which was rescued by *mrGem* mRNA (K), Cdt1MO (M), and *Snail1a* mRNA (Q) but not by *Gem** mRNA (L). Transplanted cells overexpressing geminin dispersed in the acceptor embryo (N), which was rescued by the coinjection of p53MO in donor embryos (P). Bars, 100 µm.

Gsc was completely lost when a high dose of *geminin* mRNA was injected (Fig. 2 E), whereas a low dose of *geminin* mRNA and Cdt1MO led to an expanded *gsc* domain with the anterior boundary comparable with control (Fig. 2, F and G).

To further investigate the effects of cell cycle modulations on mesendodermal cell movements, prechordal mesendodermal precursor cells from the embryonic shield of cell cycle–modulated and control (ConMo injected) donor embryos were cotransplanted into the embryonic shield of a wild-type acceptor embryo. Positions of transplanted cells were subsequently examined at the end of gastrulation (Fig. 2 I and Table S4). In contrast to the control prechordal mesendodermal cells that migrated anteriorly to the animal pole, migration of cells with decreased geminin expression was strongly delayed (Fig. 2 J). This mispositioning of prechordal plate cells coincided with the shortened anterior-posterior axis at the bud stage (Fig. 2 B) and cyclopia/synophthalmia or decreased interoptic distance phenotypes at 36 h postfertilization (hpf) in embryos injected with GemMO (Fig. S4). The aberrant positioning of transplanted cells caused by GemMO was rescued by coinjection of either *mrGem* mRNA or Cdt1MO but not *Gem** mRNA (Fig. 2, K–M). Transplanted geminin-overexpressing cells lost axial prechordal mesendodermal cell characteristics and were dispersed in the acceptor embryos (Fig. 2 N), which is consistent with the loss of *gsc* in embryos overexpressing geminin (Fig. 2 E). If the cell cycle of donor cells was modulated by injection of p21MO, delayed movements of transplanted cells were also observed (Fig. 2 O). Collectively, these data suggest that alterations of the cell cycle change mesendodermal cell movements during gastrulation.

Cell delamination is the initial step of mesendodermal cell movements during gastrulation. To test whether modulations of the cell cycle change mesendodermal cell movements during delamination, cell delamination within the embryonic shield and subsequent movements were visualized by live cell imaging. In embryos injected with ConMO, cells delaminated and moved toward both the epiblast layer and the animal pole (Video 1 and Table S1). In contrast, although cells within the delamination region in embryos injected with GemMO still moved toward the epiblast layer at a reduced velocity, many of them could not efficiently delaminate and thus moved toward the vegetal pole together with the epiblasts (Video 2 and Table S2). These results suggest that modulations of the cell cycle led to defective cell delamination at the marginal zone, therefore changing mesendodermal cell movements as shown in the cotransplantation assay (Fig. 2 J).

The cell cycle coordinates mesendodermal cell movements through apoptosis, NF-κB, and its direct downstream target, Snail1a

To investigate the mechanism through which the cell cycle coordinates mesendodermal cell movements during gastrulation, apoptosis in embryos with modulated cell cycles was examined by TUNEL assay. In comparison with the number of mitotically active cells (Fig. 1, A–H), reciprocal changes of apoptotic cell number were observed at the shield stage (Fig. 3, A–H; and Fig. S5). That is, although mitosis was positively modulated by GemMO, *Cdt1* mRNA, or p21MO (Fig. 1, B, E, and H), apoptosis was decreased (Fig. 3, B, E, and H). Similarly, when mitosis was negatively modulated by *geminin* mRNA, Cdt1MO, or MCM5MO (Fig. 1, C, D, and G), apoptosis was increased (Fig. 3, C, D, and G). If the overexpressed geminin protein lost it capability to bind to Cdt1 and cannot modulate the cell cycle (Fig. 1 F), apoptosis within the embryo remained similar to that of the control (Fig. 3 F). Furthermore, it was previously reported that inhibition of p53 can rescue the increased apoptosis caused by DNA polymerase-δ1 deficiency (Plaster et al., 2006). Coinjection of a p53MO could also rescue the increased number of apoptotic cells resulting from *geminin* mRNA expression (Fig. 3 I), indicating that apoptosis induced by *geminin* mRNA is p53 dependent.

Injection of a p65MO led to a dramatic increase of apoptosis, indicating the antiapoptotic function of p65 in gastrulating zebrafish embryos (Fig. 3 J). To investigate the response to the changed level of apoptosis resulting from cell cycle modulations, the nuclear level of antiapoptotic NF-κB was analyzed. In the nuclear phase of cells prepared from shield stage

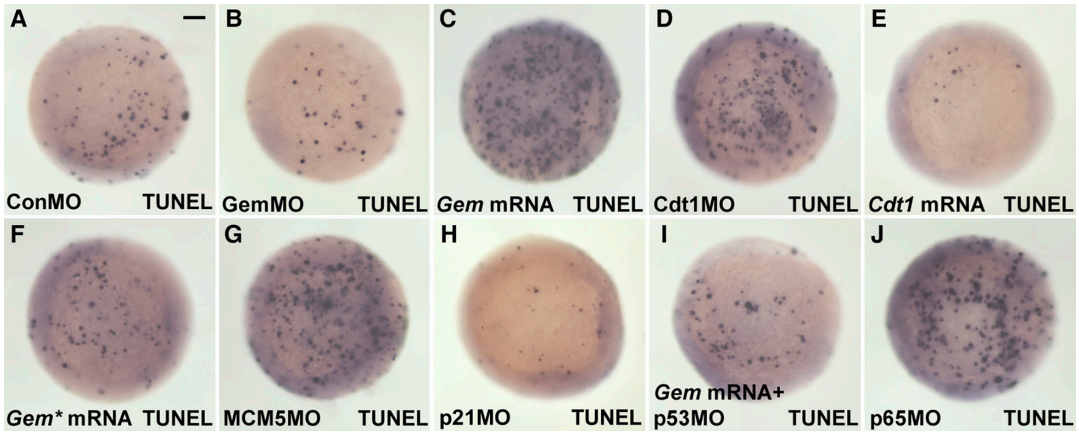

Figure 3. **Cell cycle modulations lead to changes of apoptotic level during gastrulation.** (A–H) Note that changes of the number of apoptotic cells detected by the TUNEL assay were reciprocally to those of the mitotically active cells. (I) The increased number of apoptotic cells caused by *geminin* mRNA was rescued by the coinjection of p53MO. (J) Knockdown of p65 led to an increased apoptosis. The shield stage embryos were viewed from the animal pole with the dorsal side to the right. Bar, 100 µm.

embryos injected with GemMO, *Cdt1* mRNA, or p21MO, the level of the phosphorylated active form of p65 (S276-p65) was decreased in contrast to the control (Fig. 4, A and B). In contrast, the nuclear level of S276-p65 was elevated in embryos injected with *geminin* mRNA, Cdt1MO, or MCM5MO (Fig. 4 A). The nuclear level of S276-p65 was decreased in embryos injected with p65MO, illustrating the specificity of the antibody (Fig. 4 A). In addition, if the increased apoptosis caused by *geminin* mRNA was inhibited by coinjection with p53MO (Fig. 3 I), the increased level of nuclear S276-p65 was also rescued (Fig. 4 A). These results demonstrate that the level of active antiapoptotic NF-κB corresponds to the amount of apoptosis in gastrulating embryos.

To investigate whether NF-κB is the direct upstream activator of *Snail1a* in zebrafish, a reporter construct (*Sn1-CAT*) was generated by fusion of the *Snail1a* promoter region, including the putative p65-binding site, to the chloramphenicol acetyl transferase (CAT) reporter gene. In contrast to control embryos coinjected with *Sn1-CAT* and ConMO, coinjection of *Sn1-CAT* with either p65MO or GemMO resulted in a 60–70% reduction of the CAT activity at the shield stage, whereas coinjection of *Sn1-CAT* with *p65* mRNA increased the CAT activity by about twofold (Fig. 5 A). If the putative p65-binding site was mutated in the *Sn1-CAT* reporter, the CAT activity lost its response to p65MO, GemMO, and *p65* mRNA (Fig. 5 A). To further investigate whether endogenous NF-κB directly associates with the *Snail1a* promoter region on chromatin, a chromatin immunoprecipitation (ChIP) assay was performed in shield stage embryos using antibodies against S276-p65. A DNA fragment from the *Snail1a* promoter region containing the NF-κB–binding site was coprecipitated by S276-p65 antibodies but not by preimmune serum (Fig. 5 B), indicating a direct association of NF-κB with the *Snail1a* promoter on the chromatin. As a control, a region ~1 kb downstream of the NF-κB–binding site could not be efficiently coprecipitated by S276-p65 antibodies (Fig. 5 B). These results demonstrate that in zebrafish embryos, NF-κB directly associates with the *Snail1a* promoter region on chromatin to activate transcription of *Snail1a*.

Because modulation of the cell cycle results in abnormal nuclear levels of active NF-κB and NF-κB is a direct activator of *Snail1a*, effects of cell cycle modulations on *Snail1a* were analyzed. At the shield stage, transcription of *Snail1a* in the blastoderm marginal zone, the mesendodermal precursors, was reduced in embryos with GemMO, *Cdt1* mRNA, or p21MO injected. In contrast, ectopic *Snail1a* expression was observed in embryos injected with *geminin* mRNA or MCM5MO and was more substantial in embryos injected with Cdt1MO but not *Gem** mRNA (Fig. 5, C–J). Coinjection of p53MO rescued ectopic *Snail1a* expression caused by *geminin* mRNA (Fig. 5 K), indicating that the level of *Snail1a* transcription correlates with levels of apoptosis in gastrulating embryos. Furthermore, injection of either p65MO alone or p65MO plus *geminin* mRNA led to a dramatic reduction of *Snail1a* transcription (Fig. 5, L and M), indicating that NF-κB is required for the activation of *Snail1a* and coordinates the cell cycle with *Snail1a* transcription.

To investigate whether the cell cycle coordinates mesendodermal cell movements by regulating apoptosis and Snail1a expression, *geminin* mRNA plus p53MO, or GemMO plus *Snail1a* mRNA were coinjected and mesendodermal cell movements were analyzed using the cotransplantation assay. The dispersal and incorrect position of cells caused by *geminin* mRNA and GemMO, respectively, were efficiently rescued by the coinjection of p53MO and *Snail1a* mRNA, respectively (Fig. 2, P and Q), indicating that the cell cycle coordinates mesendodermal cell movements by regulating apoptosis and Snail1a expression. Altogether, these data demonstrate that modulations of the cell cycle change apoptosis and the nuclear level of active antiapoptotic NF-κB. Through NF-κB and its direct downstream target Snail1a, the cell cycle coordinates mesendodermal cell movements during gastrulation.

Coordination of the cell cycle with mesendodermal cell movements is required for a proper distribution of mesendodermal progenitors

Gastrulation results in the formation of three germ layers. After cell delamination and subsequent migration, the newly formed hypoblast contributes to both mesoderm and endoderm. Defective cell delamination caused by manipulations of the cell cycle potentially impacts the formation of the mesendodermal layer. GemMO was observed to lead to a thinner hypoblast layer than that in the control in time lapse videos (Videos 1 and 2, yellow lines), suggesting a reduced hypoblast layer in embryos injected with GemMO.

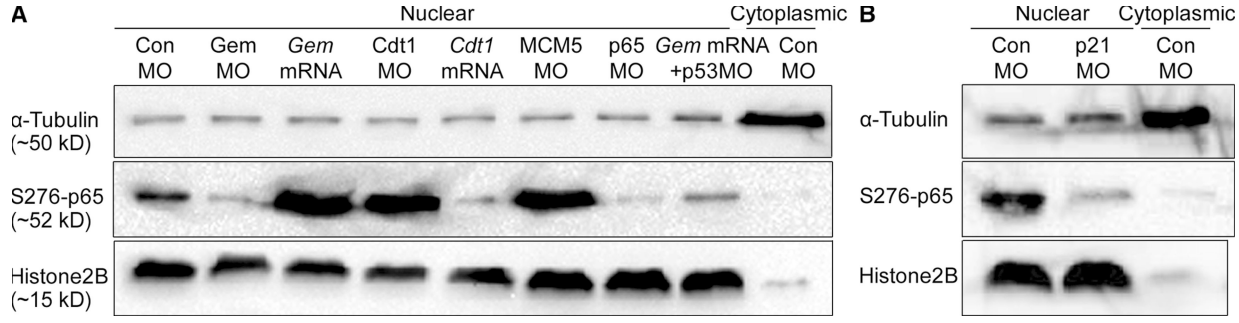

Figure 4. **Modulations of the cell cycle change the nuclear level of active p65 (S276-p65).** (A) The nuclear level of S276-p65 was reduced in embryos injected with GemMO, *Cdt1* mRNA, or p65MO, whereas it increased in embryos injected with *geminin* mRNA, Cdt1MO, or MCM5MO. The increased nuclear level of S276-p65 caused by *geminin* mRNA was rescued by the coinjection of p53MO. (B) The nuclear level of S276-p65 was reduced in embryos with p21MO. α-Tubulin served as a cytoplasmic marker, whereas histone2B served as a nuclear marker and the loading control, indicating a successful separation of nuclear and cytoplasmic phases.

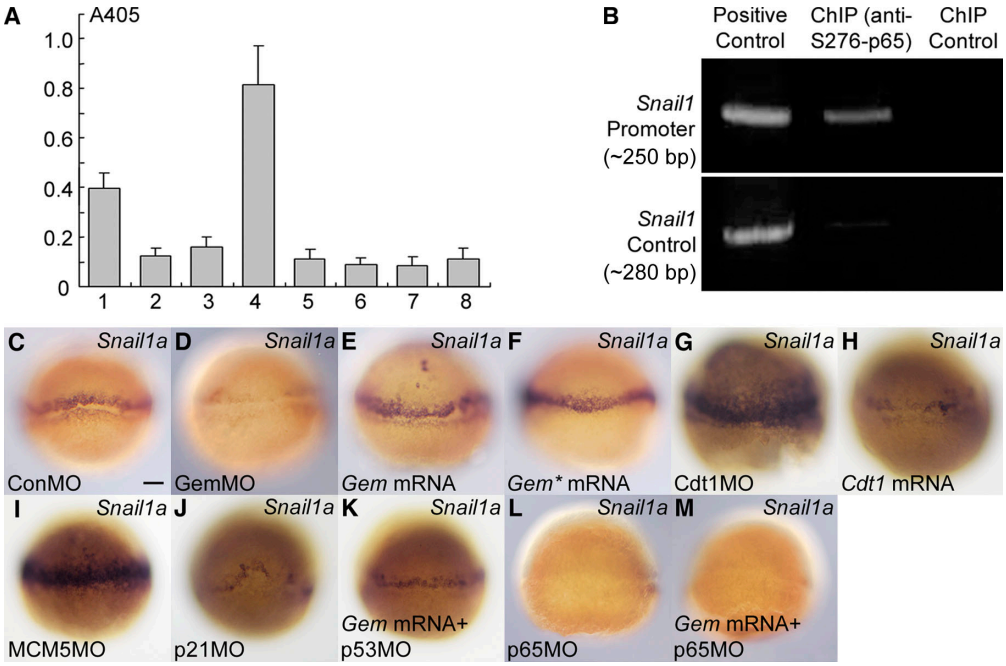

Figure 5. **Modulations of the cell cycle change the transcription of *Snail1a*, the direct downstream target of p65.** (A) p65 activates the *CAT* reporter gene driven by the *Snail1a* promoter. The following combinations were injected, and CAT activities were assayed at the shield stage: (1) *Sn1* (*Snail1a* promoter region including the NF-κB–binding site)-*CAT*+ConMO, (2) *Sn1-CAT*+p65MO, (3) *Sn1-CAT*+GemMO, (4) *Sn1-CAT+p65* mRNA, (5) *Sn1Mut* (*Snail1a* promoter region with the NF-κB–binding site mutated)-*CAT*+ConMO, (6) *Sn1Mut-CAT*+p65MO, (7) *Sn1Mut-CAT*+GemMO, and (8) *Sn1Mut-CAT+p65* mRNA. The y axis indicates the absorbance of the sample at 405 nm. Error bars indicate the standard error of six individual tests. (B) The *Snail1a* promoter region containing the NF-κB–binding site, but not a 1-kb downstream control region, was identified to associate with S276-p65 by the ChIP assay. PCR using sheared chromatin before immunoprecipitation and immunoprecipitation using preimmune serum served as positive and negative controls, respectively. (C–M) Modulations of the cell cycle change the transcription of *Snail1a* through NF-κB. Note that *Snail1a* was ectopically expressed in embryos injected with *geminin* mRNA (E), Cdt1MO (G), or MCM5MO (I), whereas it was reduced in embryos injected with GemMO (D), *Cdt1* mRNA (H), or p21MO (J). Injection of *Gem** mRNA was ineffective on the *Snail1a* transcription at the blastoderm margin (F). The ectopic expression of *Snail1a* caused by *geminin* mRNA was rescued by the coinjection of p53MO (K). Both p65MO alone (L) and *geminin* mRNA plus p65MO (M) led to a dramatic reduction of *Snail1a*. The shield stage embryos were viewed from the lateral with the shield to the right. Bar, 100 μm.

The distribution of mesendodermal cells was further examined with mesendodermal markers. *Casanova* encodes a Sox-related protein necessary and sufficient for early endoderm formation (Dickmeis et al., 2001; Kikuchi et al., 2001). At the 60% epiboly stage, the distribution of *Casanova*-expressing endodermal cells toward the animal pole was reduced by the injection of GemMO or p21MO (Fig. 6, A, B, and I). In contrast, *geminin* mRNA, Cdt1MO, or MCM5MO led to an appearance of *Casanova*-expressing cells at ectopic positions toward the animal pole, whereas *Gem** mRNA was ineffective (Fig. 6, C–E and H). In embryos overexpressing Cdt1, *Casanova* transcription was nearly lost at this stage (Fig. 6 F). Mutual rescue of the distribution of *Casanova*-expressing cells was observed between GemMO and Cdt1MO (Fig. 6 G). When p53MO was coinjected with *geminin* mRNA to inhibit the increased apoptosis, the ectopic localization of *Casanova*-expressing cells caused by *geminin* mRNA was rescued (Fig. 6 J). Furthermore, coinjection of *Snail1a* mRNA was able to rescue the reduced distribution of endodermal cells caused by GemMO, whereas *geminin* mRNA failed to induce ectopic distribution of endodermal cells in embryos with p65 knocked down (Fig. 6, K and L). Collectively, all these results demonstrate that during gastrulation, the cell cycle coordinates the distribution of endodermal cells through the apoptotic level, NF-κB, and its downstream target Snail1a.

To further study coordination of the cell cycle with the distribution of mesendodermal cells, the expression of an axial mesodermal marker *no tail* (*ntl*) was examined at the bud stage. In embryos injected with GemMO, the anterior boundary of *ntl* transcription was posteriorly shifted, concomitant with a reduced body axis (Fig. 6, M and N). In contrast, in embryos injected with *geminin* mRNA, the anterior boundary of *ntl* was anteriorly shifted, and several *ntl*-expressing cells dispersed away from the midline notochord (Fig. 6 O), which could be rescued by the coinjection of p53MO (Fig. 6 P). These results indicate that the cell cycle coordinates the distribution of axial mesodermal cells during gastrulation through the level of apoptosis.

Defective endodermal cell distributions caused by cell cycle modulation lead to a secondary effect on neural induction

Because neural induction is connected to the endodermal tissues during gastrulation (Pera et al., 1999), coordination of the cell cycle with mesendodermal cell movements implied that there may be a secondary effect on neural induction. Geminin overexpression was previously reported to induce ectopic neural tissue in *Xenopus* (Kroll et al., 1998). At the bud stage, expression of *Otx2* and *Sox2* were narrowed in embryos injected with GemMO, which was partially rescued by the coinjection of *Snail1a* mRNA (Fig. 7, A–F). To investigate whether this

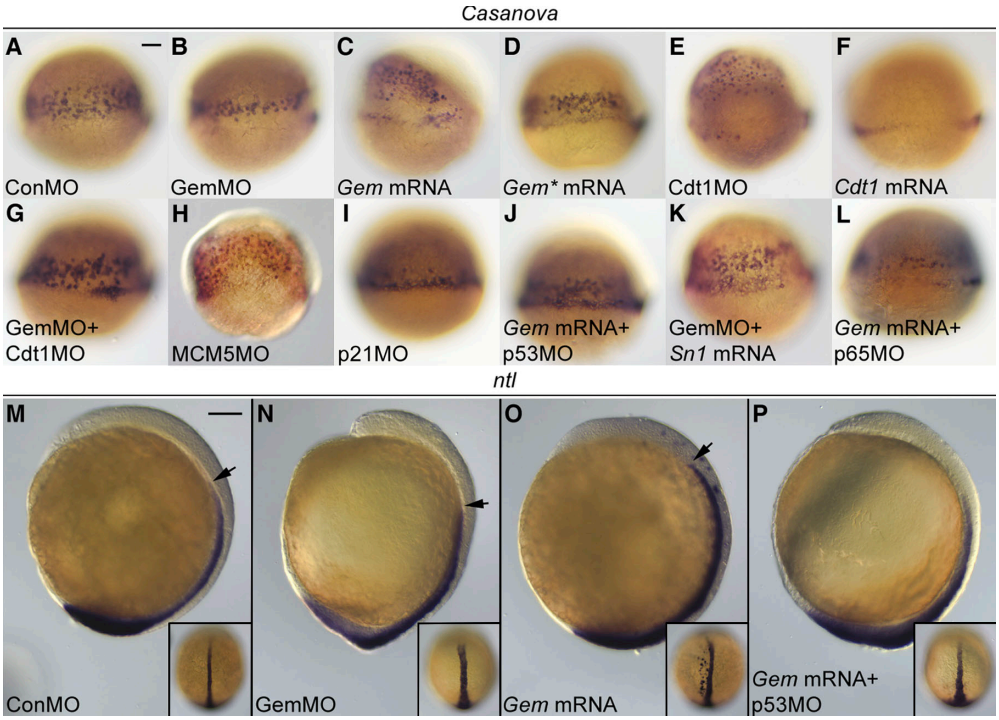

Figure 6. **The distribution of mesendodermal cells was coordinated with the cell cycle through apoptosis, NF-κB, and Snail1a.** In contrast to embryos injected with ConMO (A), distributions of the *Casanova*-expressing endodermal cells toward the animal pole were reduced in embryos injected with GemMO (B) or p21MO (I). *Geminin* mRNA (C), Cdt1MO (E), or MCM5MO (H) led to an appearance of *Casanova*-expressing cells at ectopic positions toward the animal pole, whereas *Gem** mRNA was ineffective (D). (F) *Casanova* transcription was nearly lost in embryos overexpressing Cdt1. (G) Mutual rescue of the distribution of endodermal cells between GemMO and Cdt1MO were observed. (J) The appearance of *Casanova*-expressing cells at ectopic positions toward the animal pole caused by *geminin* mRNA was rescued by the coinjection of p53MO. (K) *Snail1a* (*Sn1*) mRNA rescued the reduced movements of *Casanova*-expressing cells toward the animal pole caused by GemMO. (L) Ectopic localization of *Casanova*-expressing cells caused by *geminin* mRNA was rescued by p65MO. The 60% epiboly embryos were viewed from the lateral with the dorsal to the right. (M–P) The cell cycle coordinates with formation of the *ntl*-expressing axial mesoderm. GemMO led to a posterior shift of the anterior boundary of *ntl* transcription, concommitant with a reduced body axis (N). In embryos injected with *geminin* mRNA, the anterior boundary of *ntl* was anteriorly shifted, and several *ntl*-expressing cells dispersed away from the midline notochord (O), which was rescued by the coinjection of p53MO (P). Arrowheads mark the anterior boundary of *ntl* transcription. The bud stage embryos were viewed from lateral with the dorsal to the right. The dorsal view of each embryo is shown in the bottom right corner. Bars, 100 μm.

defective neural induction is a secondary effect of endodermal cell distribution or not, recovery of endoderm was performed by the transplantation assay. Because overexpression of Casanova is sufficient to endow endodermal cell fate (Kikuchi et al., 2001), cells from a red fluorescent donor embryo coinjected with *Casanova* mRNA plus either ConMO or GemMO were transplanted at the high stage into *cas* mutant acceptor embryos injected with GemMO. Recovery of distributions of endodermal cells was checked at the 90% epiboly stage (Fig. 7, G and H; and Table S5) and could also be confirmed at the 14 somite stage (Fig. 7, I and J; and Table S5). Embryos with successful recovery at the 90% epiboly were assayed for neural induction at the bud stage. Despite the absence of geminin in the ectoderm, *Otx2* and *Sox2* were rescued as long as distributions of Casanova-expressing endodermal cells were recovered, regardless of the donor embryo (Fig. 7, K–N). These results indicate that the defective endodermal cell distributions caused by cell cycle modulation lead to a secondary effect on neural induction.

Discussion

During the cell cycle, geminin prevents DNA resynthesis through a direct, inhibitory interaction with Cdt1. The activity of geminin is strictly controlled in different cell cycle phases. In early S phase when DNA replication is initiated, active geminin accumulates in the nucleus to bind to Cdt1 and inhibit DNA resynthesis. The presence of nuclear geminin is maintained until the end of mitosis, during which geminin is inactivated through various mechanisms such as degradation, transient polyubiquitination, and nuclear export to release Cdt1 and license the next round of the cell cycle (McGarry and Kirschner, 1998; Wohlschlegel et al., 2000; Li and Blow, 2004; Luo et al., 2007). During development, geminin regulates axial patterning, eye development, and neurogenesis through direct interactions with homeobox transcription factors and chromatin remodeling proteins (Del Bene et al., 2004; Luo et al., 2004; Seo et al., 2005). The competition between geminin–Cdt1 and geminin–homeodomain interactions suggests that geminin could function as a molecular link between the cell cycle and cell differentiation (Del Bene et al., 2004; Li and Rosenfeld, 2004; Luo and Kessel, 2004; Luo et al., 2004; Pitulescu et al., 2005). However, this competition does not seem to regulate mesendodermal cell delamination and movements addressed here. Among Hox proteins expressed during gastrulation in zebrafish, only Hoxb1b was found able to directly bind to geminin (unpublished data). In the gastrulating zebrafish embryo,

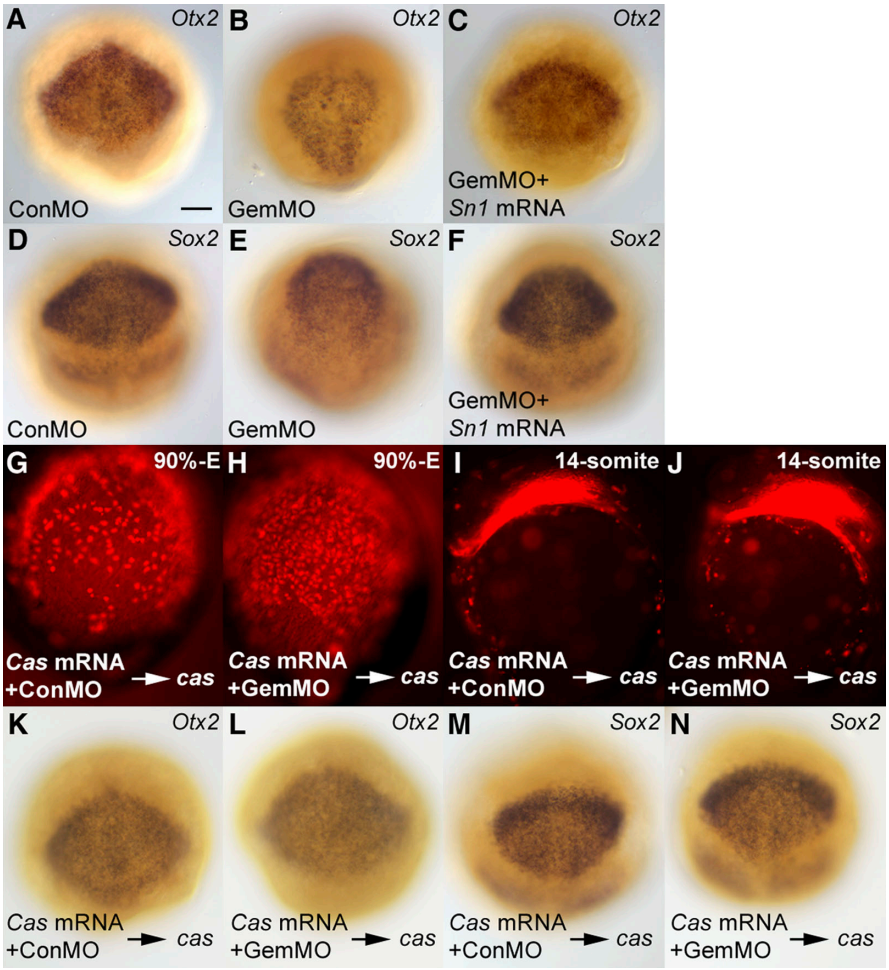

Figure 7. **Defective endodermal cell distributions caused by cell cycle modulation lead to a secondary effect on neural induction.** (A–F) At the bud stage, the narrowed expression of *Otx2* and *Sox2* caused by GemMO (B and E) was rescued by *Snail1a* (*Sn1*) mRNA (C and F). (G–J) Transplanted Casanova-overexpressing red donor cells containing ConMO (G and I) or GemMO (H and J) recover distributions of endodermal cells in the *cas* mutant acceptor embryo at both the 90% epiboly (G and H) and the 14 somite stages (I and J). The 14 somite stage embryos were viewed from the lateral with the dorsal side to the right. (K–N) At the bud stage, *Otx2* (K and L) and *Sox2* (M and N) are rescued in the *cas* mutant embryo with distributions of Casanova-expressing cells recovered, regardless of the donor embryo injected with ConMO (K and M) or GemMO (L and N). E, epiboly. Bar, 100 µm.

Hoxb1b is expressed in the presumptive hindbrain, whereas *Six3* is expressed in the anterior presumptive neural plate (Hong et al., 2008). As neither is expressed in the marginal zone or in mesendodermal cells, they lack the spatial capability to regulate mesendodermal cell movements. In this study, we took advantage of the cell cycle controlling geminin–Cdt1 balance to establish a system to manipulate the cell cycle in early zebrafish embryos. Stable changes of the number of mitotically active cells at different time points of gastrulation (shield, 70% epiboly, and 90% epiboly; Fig. 1, A–H, and not depicted) indicated the ability to positively or negatively manipulate the cell cycle in gastrulating embryos. Similar cell cycle regulatory effects were also observed at later stages in the medaka fish (Del Bene et al., 2004). In the medaka fish, injection of *geminin* mRNA has been shown to lead to cyclopia/synophthalmia (Del Bene et al., 2004), which were phenotypes resulting from GemMO injection in our work. However, these data are not contradictory. Two eye fields are separated by the prechordal plate mesodermal tissue. In embryos injected with either GemMO or *geminin* mRNA, gastrulation movements of prechordal plate cells are both defective (Fig. 2, C–E, J, and N).

In this study, reciprocal changes between the number of mitotically active cells and that of apoptotic cells were observed (Figs. 1 and 3). However, this reciprocal change could not be seen after gastrulation. Embryos injected with either GemMO or Cdt1MO, either geminin *mRNA* or *Cdt1* mRNA, all revealed an increased apoptosis at the 18 somite stage (not depicted). Similarly, embryos injected with p21MO showed a decreased number of H3P-positive cells and an increased number of apoptotic cells at the somitogenesis stage (not depicted). Two reasons could explain this discrepancy. First, it could be that after trying to keep pace with and adjust the cellular program to compensate for an abnormal cell cycle during gastrulation, cells positioned within the incorrect developmental context and with an altered intracellular program undergo apoptosis to protect the overall shape of the embryo. Alternatively, the molecular coordination between the cell cycle, apoptosis, and cell movements is perhaps not absolutely required and could potentially switch to another regulatory mechanism after gastrulation. Therefore, the mitotic and apoptotic indices may not be coordinated in developmental stages after gastrulation.

Apoptosis is only observed after gastrulation in most vertebrates, and subsequently, a proper level of apoptosis is critical for embryonic development (Negron and Lockshin, 2004; Penaloza et al., 2006). Our data suggest an explanation for why apoptosis only begins after gastrulation. A proper level of apoptosis is a determinant for the level of nuclear active NF-κB that is in turn required for Snail1a activation and cell delamination. To correctly regulate apoptosis, antiapoptotic machinery including the nuclear active NF-κB must be adjusted to compensate for ectopic or insufficient apoptosis caused by modulations of

the cell cycle (Fig. 4). The dual function of NF-κB is important for the coordination of the cell cycle with mesendodermal cell movements. NF-κB both activates antiapoptotic factors in response to apoptosis and activates *Snail1a* transcription, which is critical for mesendodermal cell delamination. Snail1a was proven to be the key coordinator downstream of NF-κB because it could rescue both delayed cell movements in the cotransplantation assay and defective distribution of mesendodermal cells caused by GemMO (Fig. 2 Q and Fig. 6 K).

Mesendodermal cell movements are initiated by a cell delamination process followed by cell migration. *Snail1a* was previously reported to be expressed in the marginal zone that is the delaminating region, the adaxial cells, and the yolk syncitial layer, but not in the migrating mesendodermal cells (Blanco et al., 2007). Our cotransplantation data showed that the cell cycle cell autonomously coordinated with cell movements (Fig. 2, J, N, and O), whereas Snail1a was able to cell autonomously rescue the defective movements caused by the cell cycle modulation (Fig. 2 Q). In addition, our time lapse videos clearly indicated defective cell delamination caused by GemMO (Videos 1 and 2). Therefore, we conclude that cell delamination is one of the steps at which the cell cycle coordinates mesendodermal cell movements. Nevertheless, it is also possible that modulations of the cell cycle change the expression of Snail1a in the yolk syncitial layer, thus contributing partially to the defective mesendodermal cell movements in a cell nonautonomous way.

Injection of *geminin* mRNA and Cdt1MO result in similar cell cycle alteration phenotypes. Although their phenotype of *gsc* transcription at the 80% epiboly stage at first appeared distinct (Fig. 2, E and G), both injections actually resulted in similar *gsc* phenotypes. Although injection of Cdt1MO led to an expansion of *gsc* transcription (Fig. 2 G) or an increased tendency for dispersion, the phenotype resulting from *geminin* mRNA presented a bona fide dispersion of cells, thus losing their identity as axial prechordal plate precursors (Fig. 2, E and N). This assumption was further proven by the injection of a lower concentration of *geminin* mRNA, which led to an expansion of *gsc* similar to embryos injected with Cdt1MO (Fig. 2, F and G).

In *Drosophila*, the cell cycle of mesodermal progenitors needs to be inhibited to allow the cell shape changes and mesodermal development (Grosshans and Wieschaus, 2000; Seher and Leptin, 2000). In this study, we showed similar results in zebrafish. An artificial positive modulation of the cell cycle by GemMO, *Cdt1* mRNA, or p21MO led to delayed or reduced distribution of mesendodermal cells, and a negative modulation of the cell cycle led to ectopic distribution or dispersion of mesendodermal cells during gastrulation (Fig. 6). If distributions of Casanova-expressing endodermal cells were recovered during gastrulation, the neural markers were restored even though ectodermal geminin was still absent (Fig. 7, G–N). This result suggests that the previously reported regulatory role of geminin on neural development (Kroll et al., 1998) may act, at least partially, as a secondary effect of mesendodermal cell movements.

In summary, we propose that in gastrulating embryos, cell cycle progression correlates with the level of apoptosis, which coincides to the correct activity of antiapoptotic machineries, including the nuclear level of active NF-κB. The dual functional NF-κB activates not only antiapoptotic factors in response to apoptosis but also Snail1a, critical for mesendodermal cell delamination, thus coordinating the cell cycle with mesendodermal cell movements during gastrulation.

Materials and methods

Zebrafish strain and maintenance

Zebrafish (*Danio rerio*) of the AB genetic background was maintained, raised, and staged as described previously (Westerfield, 2007).

cDNA isolation and mutagenesis

cDNAs encoding full-length geminin, Cdt1, and mrGem were amplified from a cDNA library prepared from the shield stage zebrafish embryos using DNA polymerase (PfuTurbo; Agilent Technologies) and primers (geminin: 5′-GTGAAGCGAGCGATTGTATTCTG-3′ and 5′-GCGGTTTTCAGTTCACTCTCATG-3′; Cdt1, 5′-CGCAGAGTAGTGCAGGGATCTC-3′ and 5′-GCACATGGTATGGTCTCAATTGTC-3′; mrGem, 5′-CAAGTATGTCAAGCATTAGGAGGCCCAAGAATGCAGAAAACCCGTCTG-3′ and 5′-GCGGTTTTCAGTTCACTCTCATG-3′; underlining indicates nucleotide exchanges relative to the wild-type geminin). The resulting fragments were cloned into pCRII-TOPO vector (Invitrogen). *Gem** was amplified using *mrGem* as a template, the primers 5′-GTGTTCTCCAGGCGGCTGCAAAGTTGGCTGCAGACATTGAAGCC-3′ and 5′-GGCTTCAATGTCTGCAGCCAACTTTGCAGCCGCCTGGAGAACAC-3′, and QuikChange Site-Directed Mutagenesis kit (Agilent Technologies) as described by the manufacturer.

Morpholinos and mRNAs

Antisense ATG morpholinos (Gene Tools) against both maternal and zygotic *geminin* (GemMO, 5′-CTTTGGTCTTCTGATGGAACTCATA-3′), *Cdt1* (Cdt1MO, 5′-CTAGATGAATGAGATCCCTGCACTA-3′), *MCM5* (MCM5MO, 5′-ATAGTTTCGATAAGTGCTGTCGATG-3′), *p65* (p65MO, 5′-CCCACTGGTGAAACATTCCGTCCAT-3′; Correa et al., 2004), *p53* (p53MO, 5′-GCGCCATTGCTTTGCAAGAATTG-3′; Langheinrich et al., 2002; Plaster et al., 2006), *p21* (p21MO, 5′-TAATAAAGAGGTCTGACCTGTGATG-3′; Sidi et al., 2008), *Snail1a* (Snail1aMO, 5′-GTCCACTCCAGTTACTTTCAGGGAT-3′), or mRNAs were injected into the yolk of one-cell stage embryos controlled by a standard ConMO (5′-CCTCTTACCTCAGTTACAATTTATA-3′). For mRNA preparation, the *geminin*, *Cdt1*, *mrGem*, *Gem**, and *Snail1a* mRNAs were synthesized from the linearized plasmid templates using the Message Machine kit (Applied Biosystems) and injected into the yolk of one-cell stage embryos. The following amounts of morpholinos or mRNAs were used for injections or rescues: 5 ng GemMO, 75 pg Cdt1MO, 2.5 ng p65MO, 1 ng p21MO, 2 ng Snail1aMO, 3 ng MCM5MO, 30 pg *geminin* mRNA, low concentration 10 pg *geminin* mRNA, 30 pg *Gem** mRNA, 150 pg *Cdt1* mRNA, 5 ng GemMO +15 pg *mrGem* mRNA, 5 ng GemMO + 30 pg *Gem** mRNA, 5 ng GemMO + 50 pg Cdt1MO, 5 ng GemMO + 25 pg *Snail1a* mRNA, 30 pg *geminin* mRNA + 150 pg *Cdt1* mRNA, 30 pg *geminin* mRNA +1 ng p53MO, and 30 pg *geminin* mRNA + 2.5 ng p65MO.

Nuclear phase isolation, CAT, and ChIP Assays

300–500 shield stage embryos were quickly deyolked in PBS, and the embryos proper were immediately incubated with 0.4 µl/embryo lysis buffer containing 40 mM Tris-HCl, pH 7.5, 150 mM NaCl, 1 mM EDTA, 0.2 mM EGTA, 15 mM NaF, 8% glycerol, and 0.4% NP-40 on ice for 5 min. The samples were spun down at 4°C for 15 min at full speed, and the supernatants were collected as cytoplasmic fractions. The pellets were washed with lysis buffer twice and sonicated in the lysis buffer to obtain the nuclear fractions. Western blottings were performed using antibodies against S276-p65 (1:50; Abcam), α-tubulin (1:4,000; Sigma-Aldrich), and histone2B (1:2,000; Millipore).

The CAT assay was performed using the CAT ELISA kit (Roche) as described by the manufacturer and previously described (Hans and Campos-Ortega, 2002). For the ChIP assay, 150–200 shield stage embryos, 400 µg S276-p65 antibodies, and two pairs of primers (*Snail1a* promoter, 5′-GATGGCACAAATGGAAACATGCTAG-3′ and 5′-CAGTCAGTTTGTAAACGTCAGGAAC-3′; *Snail1a* control, 5′-GCCTTTGCTCAAAAGCACTTATGC-3′ and 5′-GGTTTAAGTGGTTCGTGAAAGTAC-3′) were applied using the ChIP Assay kit (Millipore) as described by the manufacturer.

Whole-mount in situ hybridization, the TUNEL assay, and antibody staining

One-color whole-mount in situ hybridization was performed as described previously (Weidinger et al., 2003). The TUNEL assay was performed using In situ Cell Death Detection kit (Roche) as described by the manufacturer.

For antibody staining, embryos were fixed with 2% trichloroacetate/PBS for 2 h at room temperature and washed three times with 0.5% Triton X-100/PBS (PBTriton). After being blocked in the blocking solution (10% fetal calf serum and 0.1% bovine serum albumin in PBTriton) at 4°C overnight, embryos were incubated with antibodies against H3P (1:500; Millipore) diluted in the blocking solution at 4°C for 24 h. Then, embryos were washed six times with PBTriton for at least 15 min each and incubated with HRP–donkey anti–rabbit IgG (1:400; BioTrend) diluted in the blocking solution at 4°C overnight. After being washed six times with PBTriton for 15 min each and two times briefly with 0.5% DMSO/PBS, embryos were stained using TSA kit #5 with Alexa Fluor 594 (Invitrogen) as described by the manufacturer.

Images were captured at room temperature using AxioVision4 software (Carl Zeiss, Inc.) and a 10×/0.45 NA Plan Apochromat air objective mounted on a microscope (AxioImageZ1; Carl Zeiss, Inc.) equipped with digital cameras (MRc5 and MRm; Carl Zeiss, Inc.).

Cotransplantation, Casanova recovery, and life time imaging

Cotransplantation was performed as described previously (Yamashita et al., 2004) using 2 ng Dextran–Alexa Fluor 568 (10,000 mol wt; Invitrogen) and 0.5 ng Dextran–OregonGreen 488 (70,000 mol wt, Invitrogen) for labeling donor embryos. Images were obtained using the aforementioned setup. Bright field and fluorescent images were combined using Photoshop software (Adobe).

For Casanova recovery, donor embryos were injected with 2 ng Dextran–Alexa Fluor 568, 100 pg *Casanova* mRNA, and 5 ng ConMO or GemMO, whereas the *cas* mutant acceptor embryos were injected with 5 ng GemMO. Cells were transplanted from donor to acceptor embryos at the high stage, and the subsequent Casanova recovery was detected at the 90% epiboly stage. Time lapse videos were obtained and analyzed using a membrane GFP transgenic line (J. Topczewski, Northwestern University, Chicago, IL) as described previously (Ulrich et al., 2003, 2005).

Online supplemental material

Fig. S1 shows the amino acid sequence of zebrafish Cdt1 and geminin. Fig. S2 shows the expression pattern of geminin and Cdt1 in zebrafish embryos. Fig. S3 shows the working efficiency of GemMO and Cdt1MO as well as the binding affinity of Gem* to Cdt1. Fig. S4 shows the phenotypes caused by GemMO at 36 hpf. Fig. S5 shows the statistics of the number of TUNEL-positive cells in each embryo. Video 1 shows cell movements within delamination region of an embryo injected with ConMO. Video 2 shows cell movements within delamination region of an embryo injected with GemMO. Table S1 shows the raw data of random cell tracing in time lapse videos of embryos injected with ConMO. Table S2 shows the raw data of random cell tracing in time lapse videos of embryos injected with GemMO. Table S3 shows the statistics of phenotypes and in situ hybridizations. Table S4 shows the statistics of cotransplantation assays. Table S5 shows the statistics of the recovery of Casanova-expressing experiments.

We thank Dr. Carl-Philipp Heisenberg and Dr. Laurel Rohde for help on the two-photon microscopy, Dr. Jürg Stebler, Dr. Anming Meng, and Dr. Didier Y. R. Stainier for invaluable discussions and suggestions, Dr. Joachim Wittbrodt for protocols, Kelong Han and Julia Dörries for technical support, and Naiqing Song, Dr. Michael Kessel, and Dr. Erez Raz for continuous support.

This work was supported by the National Natural Science Foundation of China (grants 90608002 and 30700406), the National Basic Research Program of China (grants 2009CB941200 and 2007CB947100), the Program for New Century Excellent Talents (grant NCET-07-0713), the Fok Ying Tung Education Foundation (grant 111020), the Program for Changjiang Scholars and Innovative Research Team in University, the Natural Science Foundation Project of the Chongqing Science and Technology Commission (2007BB5375), and a Southwestern University grant (SWUB2008020).

Submitted: 12 June 2008
Accepted: 24 February 2009

References

Bell, S.P., and A. Dutta. 2002. DNA replication in eukaryotic cells. *Annu. Rev. Biochem.* 71:333–374.

Blanco, M.J., A. Barrallo-Gimeno, H. Acloque, A.E. Reyes, M. Tada, M.L. Allende, R. Mayor, and M.A. Nieto. 2007. Snail1a and Snail1b cooperate in the anterior migration of the axial mesendoderm in the zebrafish embryo. *Development.* 134:4073–4081.

Correa, R.G., V. Tergaonkar, J.K. Ng, I. Dubova, J.C. Izpisua-Belmonte, and I.M. Verma. 2004. Characterization of NF-kappa B/I kappa B proteins in zebra fish and their involvement in notochord development. *Mol. Cell. Biol.* 24:5257–5268.

Del Bene, F., K. Tessmar-Raible, and J. Wittbrodt. 2004. Direct interaction of geminin and Six3 in eye development. *Nature.* 427:745–749.

Dickmeis, T., P. Mourrain, L. Saint-Etienne, N. Fischer, P. Aanstad, M. Clark, U. Strahle, and F. Rosa. 2001. A crucial component of the endoderm formation pathway, CASANOVA, is encoded by a novel sox-related gene. *Genes Dev.* 15:1487–1492.

Grosshans, J., and E. Wieschaus. 2000. A genetic link between morphogenesis and cell division during formation of the ventral furrow in *Drosophila*. *Cell.* 101:523–531.

Hans, S., and J.A. Campos-Ortega. 2002. On the organisation of the regulatory region of the zebrafish deltaD gene. *Development.* 129:4773–4784.

Hong, S.K., M. Tsang, and I.B. Dawid. 2008. The mych gene is required for neural crest survival during zebrafish development. *PLoS ONE.* 3:e2029.

Ip, Y.T., and T. Gridley. 2002. Cell movements during gastrulation: snail dependent and independent pathways. *Curr. Opin. Genet. Dev.* 12:423–429.

Ip, Y.T., R.E. Park, D. Kosman, K. Yazdanbakhsh, and M. Levine. 1992. dorsal-twist interactions establish snail expression in the presumptive mesoderm of the *Drosophila* embryo. *Genes Dev.* 6:1518–1530.

Jiang, J., D. Kosman, Y.T. Ip, and M. Levine. 1991. The dorsal morphogen gradient regulates the mesoderm determinant twist in early *Drosophila* embryos. *Genes Dev.* 5:1881–1891.

Kikuchi, Y., A. Agathon, J. Alexander, C. Thisse, S. Waldron, D. Yelon, B. Thisse, and D.Y. Stainier. 2001. casanova encodes a novel Sox-related protein necessary and sufficient for early endoderm formation in zebrafish. *Genes Dev.* 15:1493–1505.

Kroll, K.L., A.N. Salic, L.M. Evans, and M.W. Kirschner. 1998. Geminin, a neuralizing molecule that demarcates the future neural plate at the onset of gastrulation. *Development.* 125:3247–3258.

Langheinrich, U., E. Hennen, G. Stott, and G. Vacun. 2002. Zebrafish as a model organism for the identification and characterization of drugs and genes affecting p53 signaling. *Curr. Biol.* 12:2023–2028.

Lee, C., B. Hong, J.M. Choi, Y. Kim, S. Watanabe, Y. Ishimi, T. Enomoto, S. Tada, Y. Kim, and Y. Cho. 2004. Structural basis for inhibition of the replication licensing factor Cdt1 by geminin. *Nature.* 430:913–917.

Li, A., and J.J. Blow. 2004. Non-proteolytic inactivation of geminin requires CDK-dependent ubiquitination. *Nat. Cell Biol.* 6:260–267.

Li, X., and M.G. Rosenfeld. 2004. Transcription: origins of licensing control. *Nature.* 427:687–688.

Luo, L., and M. Kessel. 2004. Geminin coordinates cell cycle and developmental control. *Cell Cycle.* 3:711–714.

Luo, L., X. Yang, Y. Takihara, H. Knoetgen, and M. Kessel. 2004. The cell-cylce regulator geminin inhibits Hox function through direct and polycomb-mediated interactions. *Nature.* 427:749–753.

Luo, L., Y. Uerlings, N. Happel, N.S. Asli, H. Knoetgen, and M. Kessel. 2007. Regulation of geminin functions by cell cycle dependent nuclear-cytoplasmic shuttling. *Mol. Cell. Biol.* 27:4737–4744.

Lutzmann, M., D. Maiorano, and M. Méchali. 2006. A Cdt1-geminin complex licenses chromatin for DNA replication and prevents rereplication during S phase in *Xenopus*. *EMBO J.* 25:5764–5774.

McGarry, T.J., and M.W. Kirschner. 1998. Geminin, an inhibitor of DNA replication, is degraded during mitosis. *Cell.* 93:1043–1053.

Melixetian, M., and K. Helin. 2004. Geminin: a major DNA replication safeguard in higher eukaryotes. *Cell Cycle.* 3:1002–1004.

Montero, J.A., and C.P. Heisenberg. 2004. Gastrulation dynamics: cells move into focus. *Trends Cell Biol.* 14:620–627.

Negron, J.F., and R.A. Lockshin. 2004. Activation of apoptosis and caspase-3 in zebrafish early gastrulae. *Dev. Dyn.* 231:161–170.

Penaloza, C., L. Lin, R.A. Lockshin, and Z. Zakeri. 2006. Cell death in development: shaping the embryo. *Histochem. Cell Biol.* 126:149–158.

Pera, E., S. Stern, and M. Kessel. 1999. Ectodermal patterning in the avian embryo: epidermis versus neural plate. *Development.* 126:63–73.

Pitulescu, M., M. Kessel, and L. Luo. 2005. The regulation of embryonic patterning and DNA replication by geminin. *Cell. Mol. Life Sci.* 62:1425–1433.

Plaster, N., C. Sonntag, C.E. Busse, and M. Hammerschmidt. 2006. p53 deficiency rescues apoptosis and differentiation of multiple cell types in zebrafish flathead mutants deficient for zygotic DNA polymerase delta1. *Cell Death Differ.* 13:223–235.

Saxena, S., and A. Dutta. 2005. Geminin-Cdt1 balance is critical for genetic stability. *Mutat. Res.* 569:111–121.

Saxena, S., P. Yuan, S.K. Dhar, T. Senga, D. Takeda, H. Robinson, S. Kornbluth, K. Swaminathan, and A. Dutta. 2004. A dimerized coiled-coil domain and an adjoining part of geminin interact with two sites on Cdt1 for replication inhibition. *Mol. Cell.* 15:245–258.

Seher, T.C., and M. Leptin. 2000. Tribbles, a cell cycle brake that coordinates proliferation and morphogenesis during *Drosophila* gastrulation. *Curr. Biol.* 10:623–629.

Seo, S., A. Herr, J.W. Lim, G.A. Richardson, H. Richardson, and K.L. Kroll. 2005. Geminin regulates neuronal differentiation by antagonizing Brg1 activity. *Genes Dev.* 19:1723–1734.

Sidi, S., T. Sanda, R.D. Kennedy, A.T. Hagen, C.A. Jette, R. Hoffmans, J. Pascual, S. Imamura, S. Kishi, J.F. Amatruda, et al. 2008. Chk1 suppresses a caspase-2 apoptotic response to DNA damage that bypasses p53, Bcl-2, and caspase-3. *Cell.* 133:864–877.

Stern, C. 2004. Gastrulation: From Cells to Embryo. Cold Spring Harbor Laboratory Press, Cold Spring Harbor, NY. 731 pp.

Tada, S., A. Li, D. Maiorano, M. Méchali, and J.J. Blow. 2001. Repression of origin assembly in metaphase depends on inhibition of RLF-B/Cdt1 by Geminin. *Nat. Cell Biol.* 3:107–113.

Ulrich, F., M.L. Concha, P.J. Heid, E. Voss, S. Witzel, H. Roehl, M. Tada, S.W. Wilson, R.J. Adams, D.R. Soll, et al. 2003. Slb/Wnt11 controls hypoblast cell migration and morphogenesis at the onset of zebrafish gastrulation. *Development.* 130:5375–5384.

Ulrich, F., M. Krieg, E.M. Schotz, V. Link, I. Castanon, V. Schnabel, A. Taubenberger, D. Mueller, P.H. Puech, and C.P. Heisenberg. 2005. Wnt11 functions in gastrulation by controlling cell cohesion through Rab5c and E-cadherin. *Dev. Cell.* 9:555–564.

Warga, R.M., and C.B. Kimmel. 1990. Cell movements during epiboly and gastrulation in zebrafish. *Development.* 108:569–580.

Weidinger, G., J. Stebler, K. Slanchev, K. Dumstrei, C. Wise, R. Lovell-Badge, C. Thisse, B. Thisse, and E. Raz. 2003. dead end, a novel vertebrate germ plasm component, is required for zebrafish primordial germ cell migration and survival. *Curr. Biol.* 13:1429–1434.

Westerfield, M. 2007. The Zebrafish Book: A Guide for the Laboratory Use of Zebrafish (*Danio rerio*). 5th edition. University of Oregon Press, Eugene, OR.

Wohlschlegel, J.A., B.T. Dwyer, S.K. Dhar, C. Cvetic, J.C. Walter, and A. Dutta. 2000. Inhibition of eukaryotic DNA replication by Geminin binding to Cdt1. *Science.* 290:2309–2312.

Yamashita, S., C. Miyagi, T. Fukada, N. Kagara, Y.S. Che, and T. Hirano. 2004. Zinc transporter LIVI controls epithelial-mesenchymal transition in zebrafish gastrula organizer. *Nature.* 429:298–302.

Yanagi, K., T. Mizuno, Z. You, and F. Hanaoka. 2002. Mouse geminin inhibits not only Cdt1-MCM6 interactions but also a novel intrinsic Cdt1 DNA binding activity. *J. Biol. Chem.* 277:40871–40880.

Zong, W.X., L.C. Edelstein, C. Chen, J. Bash, and C. Gelinas. 1999. The prosurvival Bcl-2 homolog Bfl-1/A1 is a direct transcriptional target of NF-kappaB that blocks TNFalpha-induced apoptosis. *Genes Dev.* 13:382–387.